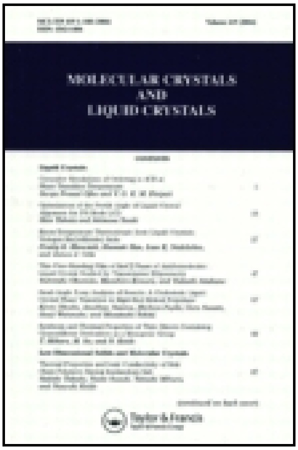

Molecular Crystals and Liquid Crystals
Publication details, including instructions for authors and subscription information:
http://www.tandfonline.com/loi/gmcl20

Fe_2O_3 Nanoparticles Coated in a SiO_2 Shell by Microemulsion Method

Ioana Lacatusu [a] , Maria Mihaly [a] , Ioan Alexandru Enesca [b] & Aurelia Meghea [a]

[a] University POLITEHNICA of Bucharest, Faculty of Applied Chemistry and Materials Science, Bucharest, Romania

[b] University Transilvania of Brasov, Product Design Centre for Sustainable Development, Brasov, Romania

To cite this article: Ioana Lacatusu, Maria Mihaly, Ioan Alexandru Enesca & Aurelia Meghea (2008): Fe_2O_3 Nanoparticles Coated in a SiO_2 Shell by Microemulsion Method, Molecular Crystals and Liquid Crystals, 483:1, 228-236

To link to this article: http://dx.doi.org/10.1080/15421400801944951

Mol. Cryst. Liq. Cryst., Vol. 483, pp. 228–236, 2008
Copyright © Taylor & Francis Group, LLC
ISSN: 1542-1406 print/1563-5287 online
DOI: 10.1080/15421400801944951

Fe_2O_3 Nanoparticles Coated in a SiO_2 Shell by Microemulsion Method

Ioana Lacatusu[1], Maria Mihaly[1], Ioan Alexandru Enesca[2], and Aurelia Meghea[1]
[1]University POLITEHNICA of Bucharest, Faculty of Applied Chemistry and Materials Science, Bucharest, Romania
[2]University Transilvania of Brasov, Product Design Centre for Sustainable Development, Brasov, Romania

Mixing elements at nanoscale range can offer exciting possibilities of novel materials with composition, structure and properties quite different from those in the bulk. Fe_2O_3 nanoparticles embedded in a surrounding silica shell were prepared via surfactant – assisted process by using dodecyl-4-lauryl ether (Brij 30) as oriented template, followed by thermal treatment. The nanoparticles are formed by the precipitation reaction of ferrous and ferric salts with ammonium hydroxide into water-in-oil microemulsion. The hydrodynamic radius of microemulsion droplets and coated nanoparticles were measured by dynamic light scattering. Their structural properties have been studied by FT-IR spectroscopy, thermogravimetric analysis and atomic force microscopy.

Keywords: Fe_2O_3 & SiO_2 nanoparticles; water-in-oil microemulsion

1. INTRODUCTION

Recently, there has been a strong research effort to obtain and manipulate the transition metal oxide nonmaterial mainly because the shape and size of the inorganic nanocrystals widely control their physical properties [1]. Fe_2O_3 nanoparticles coated in silica shell are important due to their properties, which could have promising applications in nanotechnology [2,3]. The properties of these materials

This article was supported by the Romanian National CEEX POSTDOC program, project No 8/2004. The authors gratefully acknowledge its financial support.

Address correspondence to Ioana Lacatusu, University POLITEHNICA of Bucharest, Faculty of Applied Chemistry and Materials Science, Polizu Street, No. 1, Bucharest 011061, Romania. E-mail: ioana_laca@yahoo.com

depend strongly on the particle size and the degree of dispersion of the nanoparticles in the matrix [4]. For these reasons in the present article a microemulsion method has been applied as spatially constrained nanoreactors in order to control the size of particles and to improve the monodispersity of particles synthesized. In particular, water-in-oil (reverse) microemulsions are formed by well-defined nanodroplets of the aqueous phase, dispersed by the assembly of surfactant molecules in a continuous oil phase [5]. The water-in-oil microemulsion route was chosen since it provides a unique environment to synthesize inorganic materials with interesting design and/or specific properties [6]. These nanodroplets provide a restricted reaction media to control the shape and size distribution of particles prepared by precipitating iron salts [5]. Dodecyl – 4 – lauryl ether (Brij 30) was used to obtain well – organized assemblies which provide specific sites, geometrical control and stabilization to particulate assemblies formed within the organized surfactant assemblies. The nonionic surfactant was selected since the reverse microemulsion based on nonionic surfactant is less sensitive than the ionic surfactant toward the various pH and presence of reactants in the water pools [7].

The present work aims to obtain well designed and characterized core – shell Fe_2O_3&SiO_2 nanoparticles, as well as more information about the water-in-oil microemulsion process.

2. EXPERIMENTAL

2.1. Chemicals

Chemicals were purchased from commercial sources (Fluka, Merck): polyoxyethylene-4-lauryl ether (Brij 30), isooctane, tetraethylorthosilicat (TEOS), ethanol, $FeCl_3 \cdot 6H_2O$, $FeSO_4 \cdot 7H_2O$; NH_4OH 25%. All aqueous solutions were prepared with deionised water.

2.2. Synthesis and Preparation of Samples for Various Characterisation Tests

In order to avoid any complications due to the presence of a possible thermally induced phase inversion, the reaction temperature was kept below 25°C. Two different kinds of iron oxide nanoparticles were synthesized, coated and uncoated with silica shell. For both types of synthesis the same ternary microemulsion of Brij 30/ isooctane/aqueous phase was used, but the two different procedures have been compared (Fig. 1). In the *procedure* 1, the microemulsion (μE) is prepared by mixing Brij 30 and isooctane followed by the

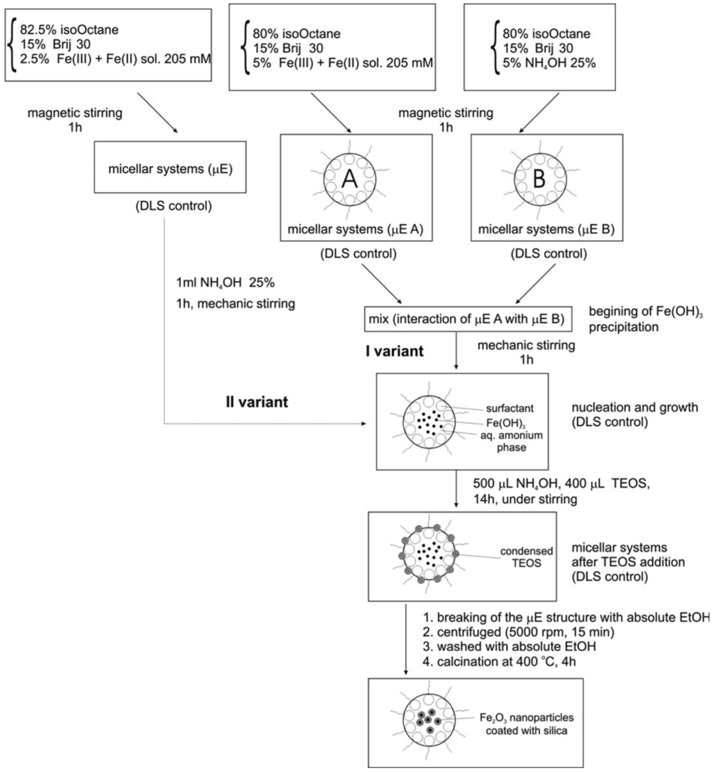

FIGURE 1 Scheme of the process with location and distribution in the reverse micelle system for both synthesis procedures.

addition in drop wise of Fe(III) + Fe(II) salts solution. The final mixture is a clear yellow μE solution. Ammonium hydroxide solution is firstly added drop wise to μE and the mixture is mechanically stirred for 1 hour. In the *procedure* 2, two microemulsions (μE A and μE B) are prepared in the same mode as in the *procedure 1*, one of them which contains as aqueous phase the Fe(III) + Fe(II) salts solution and the other NH_4OH 25%. The μE B was added drop wise to the μE A and the mixture is stirred for 1 hour. TEOS is finally added in order to obtain coated nanoparticles and the solution is mixed for 14 hours. It is possible that a fraction of TEOS molecules to remain in the bulk oil phase. Therefore, a small quantity of NH_4OH is added in order to help the TEOS hydrolysis. The amphiphilic character of hydrolysed TEOS leads to direct their location towards the droplets. There, they are distributed between the micelle cores and the water-oil interface.

Coated and uncoated samples were washed with ethanol in order to remove surfactant and oil, and were centrifuged at 5000 rpm for 15 min. The resulting powders were dried at room temperature and subjected to thermogravimetric analysis. The samples pre-sintered at 400°C in air to remove organic residues were examined by FT-IR spectroscopy. Sample preparation for nanoparticle characterisation by atomic force microscopy is relatively simple. A clean, flat glass surface has been used and the liquid microemulsion was dispersed onto a silicone substrate, followed by drying for 7 days, at 50°C. In this way the thin film was obtained to be examined for a topographic analysis by atomic force microscopy.

2.3. Measurements

The hydrodynamic diameter of microemulsion nanodroplets and uncoated/coated nanoparticles were measured by dynamic light scattering (DLS) and were performed with a Zetasizer Nano ZS from Malvern Instruments. The structure of the particles and its capping were studied by FT-IR spectroscopy and were recorded between 4000–400 cm^{-1} by Jasco 620 FT-IR. Thermogravimetric analysis (TGA) and differential thermal analysis (DTA) were performed on the dried uncoated/coated ferrous oxide in air, with Mettler Toledo TGA/SDTA 851 equipment; all the measurements were carried out from 25° up to 1000°C, with a heating rate of 10°/min. Topographic characteristics were visualized by atomic force microscopy (AFM), with NT-MDT equipment, BL222RNTE. The film was obtained operating in a contact mode, using the silicon probe (CSG10, force constant $= 0.15$ N/m, sensor radius $= 10$ nm). The dry film is scanned in ambient air.

3. RESULTS AND DISCUSSION

3.1. Systematic Study of the Effect of Aqueous Phase Composition and TEOS Incorporation on the Colloidal Aggregates Size and Polydispersity

In a first step of this study the size of nanoparticles prepared in microemulsion has been compared for the two variants of work involving two microemulsions in I variant (Fig. 2a) and one microemulsion in II variant (Fig. 2b).

Firstly, for a specific microemulsion composition, the effects of TEOS incorporation on the colloidal aggregates size and polydispersity (Pdl) have been studied (Fig. 2). Than, how these latter properties are

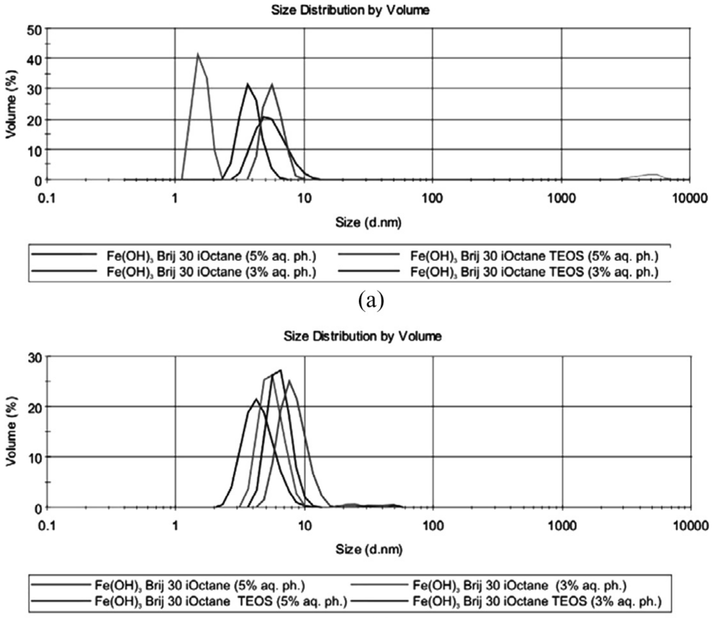

(a)

(b)

FIGURE 2 Effects of aqueous phase composition and TEOS incorporation on the size distribution for uncoated/coated $Fe(OH)_3$ nanoparticles (a = variant I, b = variant II).

dependent on the composition of the reverse microemulsion has been investigated.

With *procedure* 1 (Fig. 2a) the average diameter for uncoated particles in isooctane is 5.73 nm (93.8%, Pdl: 0.373), for 5% aqueous phase and 5.61 nm (99.8%, Pdl: 0.886), for 3% aqueous phase. A decrease in the average size is observed after TEOS incorporation as a result of shell surfactant re-organization during alcoxide hydrolysis. The average size can be decreased up to 1.59 nm (100%, Pdl: 0.046) for 5% aqueous phase. The size distribution for *procedure* 2 is similar to that of *procedure* 1, but a decrease in polydispersity for *procedure* 1 is observed.

3.2. Synthesis of Fe_2O_3 Nanoparticles Coated with Silica

The best compromise in order to get the smallest size aggregates with the lowest polydispersity is to prepare the coated/uncoated iron oxide nanoparticles by using the first procedure presented above.

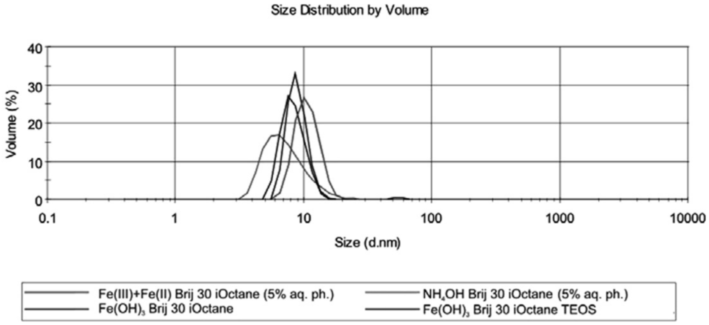

FIGURE 3 Size distribution by volume for initial microemulsions and uncoated/coated nanoparticles.

Preliminary measurements by dynamic light scattering of the droplet size distribution in both initial microemulsions (with iron salts and ammonium hydroxide as aqueous phase) are reported in Figure 3. The average hydrodynamic diameters of uncoated and coated particles are 8.90 nm (99.3%) and 8.41 nm (99.2%) respectively.

Infrared spectroscopy (Fig. 4) provides a simple tool to get some structural information of iron oxide nanoparticles. The presence of broad bands at 3419 cm^{-1}/3444 cm^{-1} and 1623 cm^{-1}/1648 cm^{-1} in uncoated/coated iron oxide nanoparticles is assigned to the presence of adsorbed water in both samples.The FT-IR spectra of coated particles (Fig. 4a) present the characteristic peaks for the Si–O–Si bond

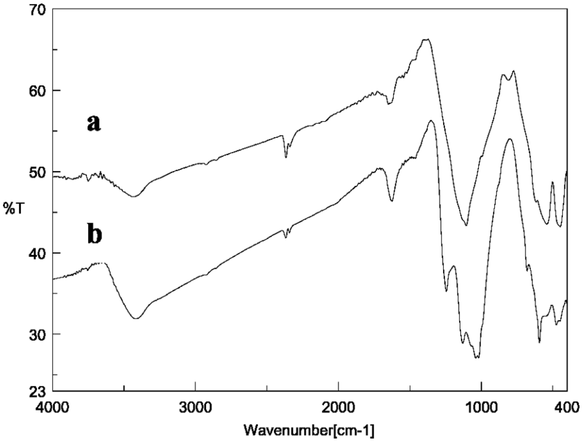

FIGURE 4 FT-IR spectra for coated (a) and uncoated Fe_2O_3 nanoparticles (b).

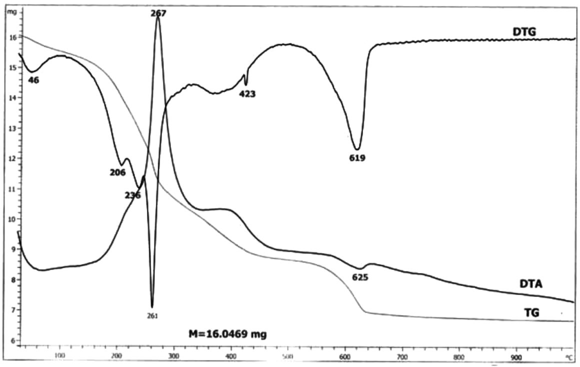

FIGURE 5 TGA curves for uncoated Fe_2O_3 nanoparticles.

($\nu_{sym\ Si-O-Si} = 806\,cm^{-1}$) and Fe–O bond ($\nu_{Fe-O} = 541\,cm^{-1}$). The sharpened peak for Fe−O bond from $592\,cm^{-1}$ (in the spectrum of uncoated particles, Fig. 4b), is substituted by a broad peak at $541\,cm^{-1}$ in the coated particle spectrum (Fig. 4a). The bands to $474\,cm^{-1}$ and $449\,cm^{-1}$ (Fig. 4b) assigned to ν_{Fe-O} are substituted in the spectrum of coated particles (Fig. 4a) with a broad band at $447\,cm^{-1}$ which is assigned to δ_{O-Si-O}. These observations lead to the supposition that the characteristic peaks for Fe−O bond can be overlapped by $\delta_{Si-O-Si}$ ($\sim 450\,cm^{-1}$). The appearance of bands at $1130\,cm^{-1}$ (uncoated particle, Fig. 4b), shifted at $1105\,cm^{-1}$ (coated particle, Fig. 4a) suggests the presence of iron and siliceous mixed oxides.

Thermogravimetric analysis was used to determine the relative composition of iron oxide core, silica shell and organic residues (or water). Figures 5 and 6 show the typical TGA and DTA curves of

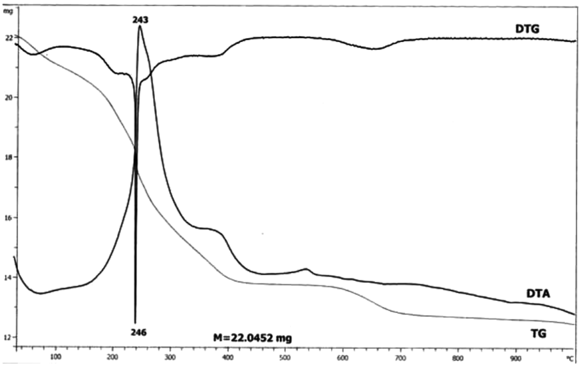

FIGURE 6 TGA curves for coated Fe_2O_3 nanoparticles.

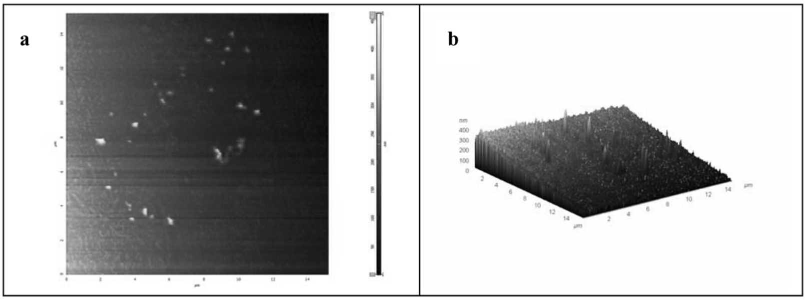

FIGURE 7 2D (a) and 3D (b) topographical scan image. Scan size is 14 × 14 micron image on thin film.

the precursors derived from microemulsions (uncoated and coated Fe_2O_3 nanoparticles). Both samples display a similar mass loss profile (DTG curves), with initial losses for water, oil, TEOS or surfactant residues. The DTA curves for both samples show a main endothermic process for each of them (267°C for uncoated and 243°C for coated particles). This temperature shift can be due to the porosity of silica shell. It can be observed a high stability of coated particles over 400°C. The higher mass loss in the case of coated particles (~22 mg) compared to the mass loss in the case of uncoated particles (~16 mg) could be explained by the combustion of organic moieties of silica shell.

The presence of the nano-sized iron oxides in silica shell was evidenced by atomic force microscopy measurements. Figure 7 is an AFM image of a microemulsion film that was dispersed onto a silicon substrate, having a few different diameters. The sample is characterised by a uniform distribution of particles, most nanoparticles show a diameter in the range 150–200 nm or less, but some agglomerates of particles are visible. From the 2D topography image, the formation of aggregates can be observed, as visible white spots. They are formed as a result of drying process of microemulsion at 50°C. The ratio of the numbers of particles at a given size is immediately apparent by visualising the 2D image (Fig. 7a).

4. CONCLUSION

Two different types of iron oxide nanoparticles were synthesized, uncoated and coated Fe_2O_3 nanoparticles, via a surfactant – assisted process, using Brij 30 as non-ionic oriented template. For both types of synthesis, the same water-in-oil microemulsion of isooctane/Brij 30/aqueous phase was used.

This study has proven that the colloidal iron - silica nanoparticles prepared in reverse microemulsion can be tailored by choosing the control level of the ammonium hydroxide (precipitating reagent for iron salts and catalyst for TEOS) and TEOS incorporation.

REFERENCES

[1] Wang, H., Zhang, J. R., & Zhu, J. J. (2002). *Journal of Crystal Growth*, *246*, 161.
[2] Abarkan, I., Doussineau, T., & Smaihi, M. (2006). *Polyhedron*, *25*, 1763.
[3] Arturo López-Quintela, M. (2003). *Current Opinion in Colloid and Interface Science*, *8*, 137.
[4] Dittert, B., Stenzel, A., & Ziegler, G. (2006). *Journal of Non-Crystalline Solids*, *352*, 5437.
[5] Vidal-Vidal, J., Rivas, J., & Lopez-Quintela, M. A. (2006). *Colloids and Surfaces A: Physicochemical and Engineering Aspects*, *288*(1–3), 44.
[6] Garcia, A., Llusar, M., Sorli, S., Calbo, J., Tena, M. A., & Monrós, G. (2003). *Journal of the European Ceramic Society*, *23*(11), 1829.
[7] Zhan, Z., Song, W., & Jiang, D. (2004). *Journal of Colloid and Interface Science*, *271*, 366.